

Adapted variable density subsampling for compressed sensing

Simon Ruetz

*University of Innsbruck
Technikerstraße 13
6020 Innsbruck, Austria*

SIMON.RUETZ@YAHOO.DE

Abstract

Recent results in compressed sensing showed that the optimal subsampling strategy should take the sparsity pattern of the signal at hand into account. This oracle-like knowledge, even though desirable, nevertheless remains elusive in most practical applications. We try to close this gap by showing how the sparsity patterns can instead be characterised via a probability distribution on the supports of the sparse signals allowing us to again derive optimal subsampling strategies. This probability distribution can be easily estimated from signals of the same signal class, achieving state of the art performance in numerical experiments. Our approach also extends to structured acquisition, where instead of isolated measurements, blocks of measurements are taken.

1. Compressed Sensing

Let $x \in \mathbb{C}^K$ be some signal and $A \in \mathbb{C}^{m \times K}$ be some matrix. Compressed sensing (CS) consists of reconstructing the signal x from measurements $y = Ax$. Usually it is assumed that the signal x is S -sparse, meaning that only $S \ll K$ elements of x are non-zero. Thus one tries to solve the following optimisation problem

$$\hat{x} = \arg \min \|x\|_1 \quad \text{s.t.} \quad y = Ax. \quad (1)$$

Starting with the seminal works [8, 14], compressed sensing theory tries to find sufficient conditions for the above minimisation problem to recover the the sparse signal. Early results suggested that if each entry of the matrix A is sampled i.i.d. from a Gaussian distribution and $m \gtrsim S \log(K)$, then the above minimisation does yield the correct solution with high probability.

These results were soon extended to a random subsampling setting, where the sensing matrix A is constructed by sampling rows a_k from a unitary matrix $A_0 \in \mathbb{C}^{K \times K}$ uniformly at random [9, 19]. In this setting, a typical sufficient condition for the above minimisation problem to recover the sparse signal with probability at least $1 - \varepsilon$ reads as

$$m \gtrsim SK \max_{1 \leq k \leq K} \|a_k\|_\infty^2 \log(K/\varepsilon). \quad (2)$$

If A_0 is the discrete Fourier matrix — for which $\max_{1 \leq k \leq K} \|a_k\|_\infty^2 = \frac{1}{K}$ — this leads to theoretical results comparable to the Gaussian setting. Nevertheless this still falls short of explaining the remarkable success of CS in most applications where $K \max_{1 \leq k \leq K} \|a_k\|_\infty^2$ is

usually quite large.

To solve this problem, variable density subsampling was introduced [19, 11, 24, 10, 20, 5]. There the sensing matrix $A \in \mathbb{C}^{m \times K}$ is constructed by sampling the rows of A_0 via a (possibly non-uniform) probability distribution. Concretely, the sensing matrix A is defined to be

$$A := \frac{1}{\sqrt{m}} \left(\frac{1}{\sqrt{\pi_{j_\ell}}} a_{j_\ell} \right)_{1 \leq \ell \leq m},$$

where m is the number of measurements we are allowed to take and j_ℓ for $1 \leq \ell \leq m$ are i.i.d random variables such that $\mathbb{P}(j_\ell = k) = \pi_k$. Note that the subsampling strategy is determined by the probabilities π_k for $1 \leq k \leq K$. A typical choice in this setting is $\pi_k := \frac{\|a_k\|_\infty^2}{\sum_k \|a_k\|_\infty^2}$ leading to the sufficient condition

$$m \gtrsim S \sum_k \|a_k\|_\infty^2 \log(K/\varepsilon).$$

This is nevertheless still not enough to completely bridge the gap between theory and application. Recent results go further by arguing that the optimal subsampling strategy should not only depend on the sensing and sparsity matrices, but also on the structure of the sparse signals [2, 6, 3]. The so called flip test proposed in [2] is a prime example of this fact. The assumption of knowledge of the structure of the sparse signals was also shown to be especially important in the case of blocks of measurements [6, 12, 3]. The drawback of all of these results is that they rely on the exact knowledge of the locations of the non-zero coefficients of the sparse signal, which may not be available in practice.

2. Contribution

In this paper we generalise these results to show how the subsampling strategy depends on the **distribution** of sparse supports together with the structure of the sensing/sparsity matrix. We are able to do this by assuming that the sparse supports follow a (possibly) non-uniform distribution, thereby generalising the aforementioned results. In practice, if one has access to a number of *similar* signals to x , a guess of the underlying distribution of sparse supports of x can be made and the optimal subsampling pattern be thus estimated. We also extend our results to the setting of structured acquisition, where instead of isolated measurements, blocks of measurements are taken. In Section 3 we introduce the relevant notation, Section 4 states the main result, Section 5 shows how to apply this result in practice and Section 6 applies our theory to some special cases to compare it to existing results. The proof of our main result is deferred to appendix A.

3. Notation and setting

A quick note on the notation used throughout this text. For an integer K , we write $\mathbb{K} := \{1, \dots, K\}$. The vectors $(e_i)_{1 \leq i \leq K}$ denote the vectors of the canonical basis of \mathbb{R}^K . For a matrix $A \in \mathbb{C}^{d \times K}$, we denote by $A_{:,k}$ (resp. $A_{k,:}$) the k -th column (resp. row) of A and by $A_{J,L}$ the submatrix with rows indexed by set $J \subseteq \{1, \dots, d\}$ and columns indexed by set $L \subseteq \mathbb{K}$. If we talk about certain columns of a matrix A , we often drop the second index,

i.e. instead of $A_{:,k}$ we will write A_k and instead of $A_{:,J}$, we will write A_J . By A^* we denote the conjugate transpose of the matrix A and by $A_k^* \in \mathbb{R}^{1 \times d}$, the conjugate transpose of the k -th column of A .

For $1 \leq p, q, r \leq \infty$ we set

$$\|A\|_{p,q} := \max_{\|x\|_q=1} \|Ax\|_p.$$

So for $B \in \mathbb{C}^{K \times m}$ we get $\|AB\|_{p,q} \leq \|A\|_{q,r} \|B\|_{r,p}$ and $\|Ax\|_q \leq \|A\|_{q,p} \|x\|_p$. Frequently encountered quantities are

$$\|A\|_{\infty,2} = \max_{k \in \{1, \dots, d\}} \|A_{k,:}\|_2 \quad \text{and} \quad \|A\|_{2,1} = \max_{k \in \{1, \dots, K\}} \|A_k\|_2,$$

which denote the maximum ℓ_2 -norm of a row and the maximum ℓ_2 -norm of a column of A respectively. Note that $\|A\|_{\infty,2} = \|A^*\|_{2,1}$. Further note that $\|A\|_{\infty,1}$ is the maximum absolute entry of the matrix A . For ease of notation we sometimes write $\|A\| = \|A\|_{2,2}$ for the operator norm which corresponds to the largest singular value of A . For a vector $v \in \mathbb{R}^d$, we denote by $\underline{v} := \|v\|_{\min} := \min_i |v_i|$ the smallest absolute entry of v and $\|v\|_{\max} := \|v\|_{\infty}$ the biggest absolute entry of v . We write $x \lesssim y$ if there exists a constant $c > 0$, such that $x \leq cy$. We write $\text{vec} : \mathbb{C}^{d \times d} \mapsto \mathbb{C}^{d^2}$ for the vectorisation operation that transforms a complex matrix into a complex vector by stacking the columns on top of each other and by vec^{-1} its inverse. Further, for any vector v we denote by D_v resp. $\text{diag}(v)$ the diagonal matrix with v on the diagonal.

As was noted in the introduction we want the supports of our signals to follow a non-uniform distribution. We are going to use the following probability measure on $\mathcal{P}(\mathbb{K})$ that allow us to model non-uniform distributions for our supports while still ensuring that they are S -sparse.

Definition 1 (Rejective sampling - Conditional Bernoulli model) *Let $0 \leq p_j \leq 1$ be such that $\sum_{j=1}^K p_j = S$. We say our supports follow the rejective sampling model, if each support $I \subseteq \mathbb{K}$ is chosen with probability*

$$\mathbb{P}(I) := \begin{cases} c \prod_{i \in I} p_i \prod_{j \notin I} (1 - p_j) & \text{if } |I| = S \\ 0 & \text{else} \end{cases}, \quad (3)$$

where c is a constant to ensure that \mathbb{P} is a probability measure. We define the $D_p := \text{diag}((p_k)_k)$ as the square diagonal matrix with the weight vector p on its diagonal. We call $W \in \mathbb{R}^{\sqrt{K} \times \sqrt{K}}$ the weight matrix, if $\text{vec}(W) = p^1$.

One important thing to note here is that in general $p_i \neq \mathbb{E}[i \in I]$ (except for the case $p_i = \frac{S}{K}$). Luckily, especially for large K , we have $p_i \approx \mathbb{E}[i \in I]$ [18, 27], which allows one to estimate the underlying probability vector p by approximating them by the probability of occurrence $\mathbb{E}[i \in I]$ which in turn can be estimated from a dataset.

Let D_I be the square diagonal *selector matrix* satisfying $(D_I)_{\ell,\ell} = 1 \Leftrightarrow \ell \in I$.

This lets us define the following model for our signals. We specify two models, one for the complex and one for the real case.

1. Here we implicitly assume that \sqrt{K} is an integer.

Definition 2 (Signal model) We model our signals as

$$x = \sum_{i \in I} e_i x_i \sigma_i, \quad (4)$$

where $x_i \in \mathbb{R}$ (or \mathbb{C}) and $I = \{i_1, \dots, i_S\}$ is the random support following the rejective sampling model with weight vector p such that $\sum_{i=1}^K p_i = S$ and denote by D_p the corresponding diagonal matrix. Further we assume that σ_i forms a Rademacher sequence.

4. Main result

Assume we are given a unitary matrix $A_0 \in \mathbb{C}^{K \times K}$ representing the set of possible linear measurements $(A_0^*)_{i \cdot} =: a_i^*$. We partition the set \mathbb{K} into M blocks \mathcal{I}_k such that $\uplus_k \mathcal{I}_k = \mathbb{K}$ and set

$$B_k := (a_i)_{i \in \mathcal{I}_k} \in \mathbb{C}^{|\mathcal{I}_k| \times K}$$

The sensing matrix A is then defined as

$$A := \frac{1}{\sqrt{m}} \left(\frac{1}{\sqrt{\pi_{j_\ell}}} B_{j_\ell} \right)_{1 \leq \ell \leq m},$$

where $m \leq M$ is the number of blocks we want to measure and j_ℓ for $1 \leq \ell \leq m$ are i.i.d random variables such that $\mathbb{P}(j_\ell = k) = \pi_k$. So the π_k define the probability with which each block of measurements is selected. In line with existing compressed sensing literature we call

$$\max_k \|a_k\|_\infty^2, \quad (5)$$

the coherence of the matrix A_0 . With these definitions we are finally able to state our main result.

Theorem 3 Assume m measurements B_k are sampled according to probabilities π_k and that the signals follow the model in 2, where the support $I \subseteq \mathbb{K}$ is chosen according to the rejective sampling model with probabilities p_1, \dots, p_K such that $\sum_{k=1}^K p_k = S$ and $0 < p_k \leq 1$. If

$$\begin{aligned} m &\gtrsim \max_k \frac{\|B_k^* B_k\|_{\infty,1}}{\pi_k} \log^3(K/\varepsilon), \\ m &\gtrsim \max_k \frac{\|B_k D_p B_k^*\|_{2,2}}{\pi_k} \log^2(K/\varepsilon), \end{aligned} \quad (6)$$

then (1) recovers the sparse signal with probability $1 - \varepsilon$.

The exact statement — including constants — can be found in Section A. The restriction $p > 0$ is no real constraint, as in the case of $p_i = 0$ for some i , a careful analysis of the proof shows that one can then set the i -th column of A to zero since this index is never part of the random supports I anyway.

Remark 4 This result also extends to signals x that are sparse in some unitary basis Ψ by a change of variable. If we denote by Φ^* our original sensing matrix and let $x = \Psi z$ for some sparse vector z , then we can again apply the above result with the new sensing matrix $A_0 = \Phi^* \Psi$ and sparse signal z . In this case, the coherence $\|a_k\|_\infty$ is similar to a cross-coherence by noting that $\|a_k\|_\infty = \max_{i,j} |\langle \phi_i, \psi_j \rangle|$.

Remark 5 Even though the above result is stated in terms of the product probability measure of measurements and signals, careful analysis of the proof shows that in fact it can also be understood in a sequential manner. When sampling the measurement matrix according to probabilities π_k (and the conditions of the theorem are satisfied), then with high probability one will get a measurement matrix that works for most signals. This is what one hopes for since the aim is usually to construct a measurement matrix that works well for multiple signals.

The above result shows that the optimal sampling strategy π should depend both on the distribution p of sparse supports via the diagonal matrix D_p and on the structure of the blocks B_k . One way to optimise the bounds is by setting

$$\pi_k := \frac{\max\{\|B_k D_p B_k^*\|_{2,2}, \|B_k^* B_k\|_{\infty,1}\}}{L}, \quad (7)$$

where L is a normalising constant ensuring $\sum_k \pi_k = 1$. By plugging this bound into the above theorem we get the sufficient condition

$$m \gtrsim \left(\sum_k \|B_k D_p B_k^*\|_{2,2} + \sum_k \|B_k^* B_k\|_{\infty,1} \right) \log^3(K/\varepsilon). \quad (8)$$

In Section 6 we will look at special cases of blocks of measurements, where this bound on m can further be simplified. For isolated measurements, i.e. the case where $B_k = a_k$, the above yields the following result.

Corollary 6 Assume that the signals follow the model in 2, where the support $I \subseteq \mathbb{K}$ is chosen according to the rejective sampling model with probabilities p_1, \dots, p_K such that $\sum_{k=1}^K p_k = S$ and $0 < p_k \leq 1$. If the measurements a_k are sampled according to

$$\pi_k = \frac{\max\{a_k D_p a_k^*, \|a_k\|_\infty^2\}}{L}, \quad (9)$$

where L is a normalising constant ensuring $\sum_k \pi_k = 1$, and if

$$m \gtrsim \left(S + \sum_k \|a_k\|_\infty^2 \right) \log^3(K/\varepsilon), \quad (10)$$

then (1) recovers the sparse signal with probability $1 - \varepsilon$.

Proof First note that $\|B_k D_p B_k^*\|_{2,2} = a_k D_p a_k^*$ and thus

$$\sum_k a_k D_p a_k^* = \text{tr}(A_0 D_p A_0^*) = \text{tr}(D_p) = S.$$

Further

$$\|B_k^* B_k\|_{\infty,1} = \|a_k^* a_k\|_{\infty,1} \leq \max_{i,j} |a_{k,i} a_{k,j}| \leq \max_i |a_{k,i}|^2 = \|a_k\|_{\infty}^2,$$

leading to $L \leq S + \sum_k \|a_k\|_{\infty}^2$. Plugging these π_k into Theorem 3 yields the result. \blacksquare

This result is an improvement upon standard results for general (unknown) supports I , which read as $m \gtrsim S \sum_k \|a_k\|_{\infty}^2 \log(K)$ [9, 24, 20, 10]. This is to be expected since we assume that information about the supports and their distribution is available. On the other hand, the additional log factors are the price we pay for our random signal approach. A comparison to existing results that assume knowledge about the structure of sparsity will be conducted in Section 6.

Further, Corollary 6 shows how, for a given weight vector p , this lower bound is attained via the formula in (9). This is an easy-to-use recipe yielding state of the art results in a number of experiments (see also Sections 6). We now show that this indeed outperforms standard subsampling procedures in numerical experiments.

5. Numerical experiments

Now we conduct a few experiments to compare the performance of our subsampling scheme to heuristically inspired subsampling schemes used in practice. For our first experiment (Figure 1) we assume a standard compressed sensing setup with isolated 2D Fourier measurements and a 2D DB4 wavelet matrix as sparsifying basis.

We assume to be given a training set of images from which we generate the sparse distribution model by transforming them into a wavelet basis before applying a threshold. The relative frequency with which each coefficient appears in these sparse supports is our proxy for the inclusion probabilities p , since for large sample sizes they are approximately equal to the expectation of an atom being in the support [18, 27]. This one-to-one correspondence is related to the close relationship between the rejective sampling model and the Bernoulli sampling model with weights p [18, 27, 26].

We further assume to be given a reference image (bottom right) which we have to reconstruct. We will compare the performance of our subsampling strategy in the isolated measurement case against a state-of-the-art variable density subsampling scheme with polynomial decay, where we pick a frequency (k_1, k_2) in the 2D k -space with probability $\frac{1}{(k_1^2 + k_2^2)^{2.5}}$. To ensure meaningful results, each experiment is averaged over 10 runs. All sampling distributions will be plotted in log-scale.

To approximate the distribution of the sparse supports, we use a dataset of around 4.000 real brain images [7] onto which we apply the 2D DB4 wavelet transform followed by a thresholding operation with a threshold of around 0.006, yielding the weight matrix W (top right). Plugging these weights into Formula (9) and normalising the resulting density to 1, we get the adapted subsampling distribution π (top left). We compare this strategy to the above mentioned polynomial decaying density (top middle) by sampling 10% of frequencies in the k -space (bottom left and middle). Finally, an application of the NESTA algorithm to solve (1) for both sets of measurements yields the results in the figure. As can be seen, the adapted subsampling strategy is able to slightly outperform the quadratically decaying subsampling strategy — resulting in a PSNR value of 23.8 compared to 32.0.

To show that our new subsampling strategy does indeed adapt to the underlying distri-

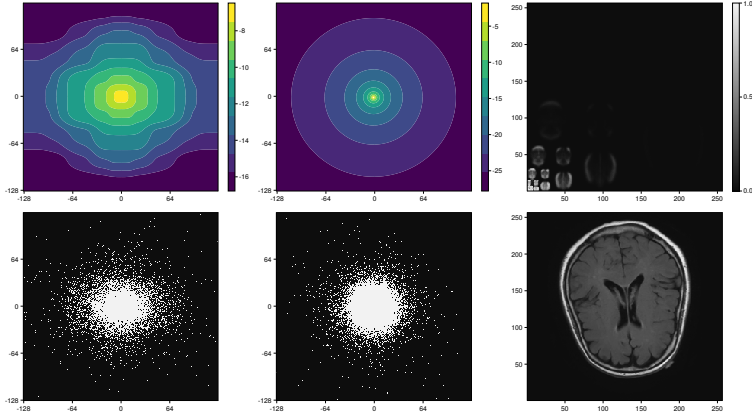


Figure 1: Adapted variable density sampling scheme (left column) vs polynomial decay (middle column). Estimated Matrix W of inclusion probabilities for the sparse support distribution in the DB4 wavelet basis (top right) and test image (bottom right). The resulting PSNR values are: Adapted - 32.8 and Polynomial - 32.0.

bution of sparse supports, we repeat the above experiment (Figure 2) but this time use a different dataset — the MRNet dataset which consists of around 30.000 images of knees [28]. To generate the matrix W we again transform each training image into the DB4 wavelet basis and apply a threshold of about 0.006 to get distribution of non-zero coefficients (top right). This time the resulting weights are non-symmetrical and hence plugging them into Formula (9) results in a non-symmetrical subsampling density, thereby *adapting* to the underlying structure of the signals. This makes the difference between the adapted subsampling distribution and the polynomial subsampling strategy more pronounced, which will also result in greater differences in the PSNR. Sampling 10% of measurements from the adapted and polynomial densities (bottom left and middle), we get by again applying the NESTA algorithm to (1) that our adapted subsampling scheme outperforms the heuristically inspired polynomial subsampling strategy — resulting in a PSNR value of 27.9 compared to 26.8.

This difference in performance gets even more pronounced in the next experiment (Figure 3), where we use the same setup (and dataset) as in the first experiment, but **flip** the sparse coefficients of each image (including the test image) by applying the transform $x \mapsto x^f \in \mathbb{C}^K$, $x_1^f = x_K, x_2^f = x_{K-1}, \dots, x_K^f = x_1$ to the vectorised sparse coefficients. This is inspired by the so-called flip test [2]. Obviously, the estimated distribution of the sparse supports is now flipped as well (top right) and plugging these weights p into Formula (9) yields a completely different sampling distribution. We again sample 10% of measurements from the 2D k-space (bottom left and middle). This time, our adapted subsampling strategy easily outperforms the heuristic polynomial decay subsampling strategy — resulting in a PSNR value of 22.7 compared to 12.0.

These experiments showed that our subsampling scheme really does adapt to the underlying distribution of sparse supports and outperforms heuristic subsampling schemes.

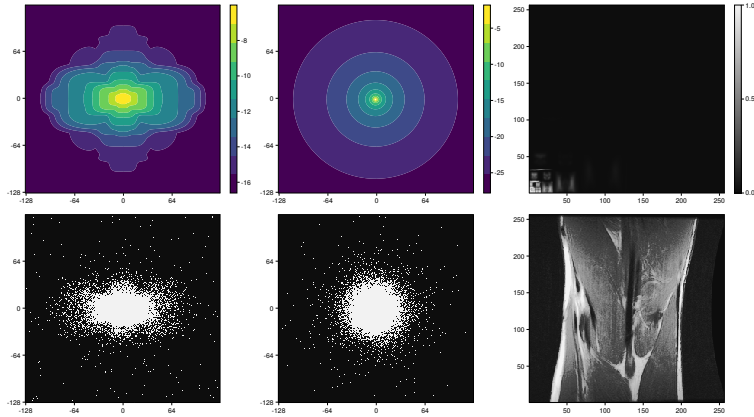


Figure 2: Adapted variable density sampling scheme (left column) vs polynomial decay (middle column). Estimated Matrix W of inclusion probabilities for the sparse support distribution in the DB4 wavelet basis (top right) and test image (bottom right). The resulting PSNR values are: Adapted - 27.9 and Polynomial - 26.8.

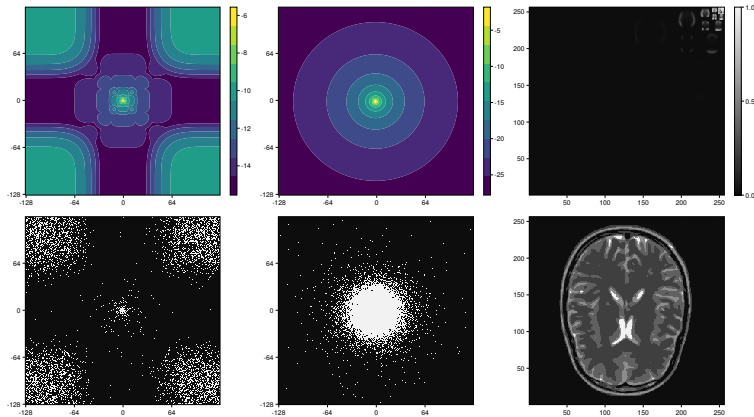


Figure 3: Adapted variable density sampling scheme (left column) vs polynomial decay (middle column). Estimated Matrix W of inclusion probabilities for the sparse support distribution in the DB4 wavelet basis (top right) and test image (bottom right). The resulting PSNR values are: Adapted - 26.4 and Polynomial - 14.0.

6. Special cases

In this section we want to analyse our result for a few special cases of measurement matrices, sparsity basis and weights p which underline the generality of the above result. We further show how our result can be applied to recover state of the art theoretical results in CS theory.

6.1 Coherent matrix

A frequent example showing the necessity of some sort of knowledge of the structure in sparse signals is the special case $A_0 = \mathbb{I}$. Denote by $J := \{i : p_i \neq 0\}$ the set of indices where the weights of our random support model are zero and set the columns of A_{J^c} to zero. In this setting, Formula (9) leads to $\pi_k = \frac{\delta_{k,J}}{|J|}$ and thus $m \gtrsim |J| \log^3(K/\varepsilon)$ which means that to ensure recovery with high probability, we have to sample all rows corresponding to positive weights p_ℓ , i.e. all those rows that correspond to entries of our sparse vector that have a non-zero probability of appearing in the support. This also includes the setting where $p \in \{0, 1\}$ recovering, up to logarithmic factors, results derived in [6] for fixed sparse supports.

6.2 Fourier matrix

Assume that $A_0 = \mathcal{F}$, i.e. A_0 is the 1-D Fourier transform. This matrix is known to be incoherent ($\|a_k\|_\infty^2 = \frac{1}{K}$) and in the isolated measurement setting our result yields $a_k D_p a_k^* = \sum_\ell |a_{k,\ell}| p_\ell \leq \|a_k\|_\infty \|p\|_1 = \frac{1}{K} \sum_\ell p_\ell = \frac{S}{K}$ for any weight vector p (recall that $\sum_\ell p_\ell = S$). Plugging these observations back into our main Theorem yields that independent of the distribution p , one should sample uniformly at random, i.e. $\pi_k = \frac{1}{K}$. Corollary 6 thus yields $m \gtrsim S \log^3(K)$ which (up to log factors) is in line with standard lower bounds on the number of measurements [8, 13].

6.3 Uniformly distributed sparse supports

One possible distribution of our sparse supports is the uniform distribution, where $p_\ell = S/K$. Plugging this into Formula (9) yields

$$\pi_k = \frac{\max\{S/K, \|a_k\|_\infty^2\}}{L},$$

where L again is a normalising constant. This improves upon to coherence based subsampling strategies [19, 11, 24], where $\pi_k := \frac{\|a_k\|_\infty^2}{\sum_\ell \|a_\ell\|_\infty^2}$. Intuitively, since in the uniform case there is no structure in the sparse signals that can influence the subsampling strategy it is only natural that in this special case the optimal subsampling strategy depends only on the structure of the sensing matrix together with a lower bound S/K to cover the whole space. To see that the our result is indeed tight in the sense that both terms in the numerator of Formula 9 are indeed necessary, we conduct a small experiment. We set $K = 2^{16}$, $S = \sqrt{K}/2$ and let Φ^* be the 2D Hadamard transform and Ψ be the 2D Haar wavelet transform. We then generate 100 synthetic signals via our signal model 2 with uniformly distributed sparse supports $p_\ell = S/K$, coefficients $c = 1$ and random signs $\sigma = \pm 1$. We then compare the performance of three different subsampling strategies π^1, π^2 and π^3 defined as

$$\pi_k^1 = \frac{\max\{S/K, \|a_k\|_\infty^2\}}{L}, \quad \pi_k^2 = \frac{m}{K}, \quad \pi_k^3 = \frac{\|a_k\|_\infty^2}{\sum_\ell \|a_\ell\|_\infty^2}. \quad (11)$$

We call them the adapted, uniform and coherence based subsampling strategies — see also top row of Figure 4. Sampling 5% of measurements from each of these distributions and subsequently solving 1 with the NESTA algorithm [23, 4] and averaging the PSNR over 10

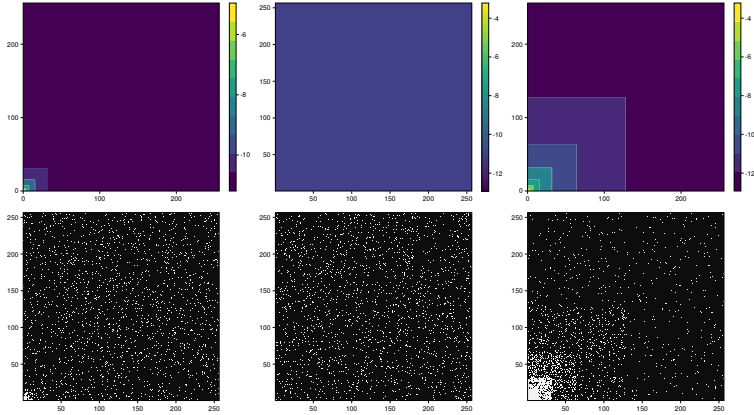


Figure 4: Subsampling densities (top row) and corresponding samples (bottom row) for the adapted variable density sampling scheme (left column), the uniform distribution (middle right) and the coherence based subsampling scheme (right row). The resulting average PSNR are: adapted - 133.5, uniform - 105.6 and coherence based- 62.3.

runs, each with 100 fresh signals, shows that our adapted subsampling strategy outperforms both the uniform and the coherence bases subsampling strategy, indicating that both terms in (11) are not only sufficient, but indeed necessary.

6.4 Sparsity in levels

A frequent assumption in modern compressed sensing theory is sparsity in levels [2, 6, 3, 1, 21]. To apply our results to this framework we assume that $K = 2^{J+1}$ for some $J \in \mathbb{N}$ and set $A_0 = \mathcal{F}\Psi^*$, where \mathcal{F} is the 1-D Fourier transform with rows indexed from $-K/2 + 1$ to $K/2$ and Ψ is the 1-D Haar wavelet transform. Denote by Ω the dyadic partition of the set $\{1, \dots, K\}$ where $\Omega_0 := 0$, $\Omega_1 := 1$ and $\Omega_j := \{2^{j-1} + 1, \dots, 2^j\}$ for $j = 2, \dots, J + 1$. Further denote by M the $J + 1$ frequency bands of the discrete Fourier transform \mathcal{F} , i.e., $M_0 := \{0, 1\}$ and $M_j := \{-2^j + 1, \dots, -2^{j-1}\} \cup \{2^{j-1} + 1, \dots, 2^j\}$ for $j = 1, \dots, J$. Lemma 1 in [1] states that for $\ell \in \Omega_i$ and $k \in M_j$

$$|a_{k,\ell}|^2 \lesssim 2^{-j} 2^{|j-i|}. \quad (12)$$

We define the **average sparsity in level** ℓ as

$$S_\ell := \|p_{\Omega_\ell}\|_1 \quad (13)$$

For simplicity we assume $S_\ell > 1$ for all $1 \leq \ell \leq J$. Plugging this into (9) yields for $k \in M_j$

$$a_k D_p a_k^* \lesssim 2^{-j} S_j + 2^{-j} \sum_{p \neq j} 2^{|j-p|} S_p, \quad (14)$$

and thus by using π as defined in (9) our main result yields the sufficient condition

$$m \gtrsim \left(\sum_j S_j + \sum_{p \neq j} 2^{|j-p|} S_p \right) \log^3(K/\varepsilon), \quad (15)$$

in line with results in [3].

6.5 Blocks of measurements

Even though the above sampling strategies yield very good reconstruction results, probing measurements independently at random is infeasible — or at least impractical — in most real applications, see [6] and references therein. Luckily, our results easily extend to the case of blocks of measurements B_k .

6.5.1 SENSING VERTICAL (OR HORIZONTAL) LINES IN 2D

We will again follow the notation in [6, 3] very closely to facilitate easier comparison. Assume again that $K = 2^{J+1}$ for some odd $J \in \mathbb{N}$. Let $A \in \mathbb{C}^{\sqrt{K} \times \sqrt{K}}$ be a unitary matrix (for example the discrete 1D Fourier-Haar transform matrix) and assume that our set of possible measurements is given by

$$A_0 = A \otimes A \in \mathbb{C}^{K \times K}, \quad (16)$$

where \otimes denotes the Kronecker product. With this notation, we define blocks of measurements which, in a 2D Fourier-Wavelet setting would correspond to vertical lines in frequency space. For this set

$$B_k := A_{k,:} \otimes A = \left(A_{k,1}A \mid \dots \mid A_{k,\sqrt{K}}A \right) \in \mathbb{C}^{\sqrt{K} \times K} \quad \text{for all } 1 \leq k \leq \sqrt{K}.$$

The separable nature of this setup has the big advantage that the matrix $B_k^* B_k$ has a very nice representation. Note that in our main result we have to control $\|B_k D_p B_k^*\| = \|D_{\sqrt{p}} B_k^* B_k D_{\sqrt{p}}\|$. Using that A is a unitary matrix we see

$$B_k^* B_k = (A_{k,:} \otimes A)^* (A_{k,:} \otimes A) = (A_{k,:}^* A_{k,:} \otimes A^* A) = (A_{k,:}^* A_{k,:} \otimes \mathbb{I}). \quad (17)$$

For our weight vector $p \in \mathbb{R}^K$ we denote by $W \in \mathbb{R}^{\sqrt{K} \times \sqrt{K}}$ the matrix satisfying $\text{vec}(W) = p$. Multiplying $B_k^* B_k = (A_{k,:}^* A_{k,:} \otimes \mathbb{I})$ from the left and right with the diagonal matrix $D_{\sqrt{p}}$ and taking the operator norm yields

$$\|D_{\sqrt{p}} (A_{k,:}^* A_{k,:} \otimes \mathbb{I}) D_{\sqrt{p}}\| = \|D_{\sqrt{p}} \begin{pmatrix} A_{k,1}^* A_{k,1} \mathbb{I} & \dots & A_{k,1}^* A_{k,\sqrt{K}} \mathbb{I} \\ \vdots & \ddots & \vdots \\ A_{k,\sqrt{K}}^* A_{k,1} \mathbb{I} & \dots & A_{k,\sqrt{K}}^* A_{k,\sqrt{K}} \mathbb{I} \end{pmatrix} D_{\sqrt{p}}\|.$$

Since reordering of columns and rows does not change the operator norm, we apply the permutation $R : \mathbb{K} \mapsto \text{vec}(\text{vec}^{-1}(\mathbb{K})^*)$ to both the columns and rows of the above matrix

and set $p' := R(p)$ to get

$$\begin{aligned} \|D_{\sqrt{p'}}(A_{k,:}^* A_{k,:} \otimes \mathbb{I})D_{\sqrt{p'}}\| &= \left\| D_{\sqrt{p'}} \begin{pmatrix} A_{k,:}^* A_{k,:} & \dots & 0 \\ \vdots & \ddots & \vdots \\ 0 & \dots & A_{k,:}^* A_{k,:} \end{pmatrix} D_{\sqrt{p'}} \right\| \\ &= \max_{1 \leq \ell \leq \sqrt{K}} \|A_{k,:} D_{W_{\ell,:}}^{1/2}\|_2^2 = \max_{1 \leq \ell \leq \sqrt{K}} \sum_{i=1}^{\sqrt{K}} |A_{k,i}|^2 W_{\ell,i}. \end{aligned}$$

So we look for the row v of the matrix W , such that $\|A_{k,:} D_{\sqrt{v}}\|_2^2$ is maximised. This encapsulates the relationship between the structure of the blocks of measurements and the structure of the sparse signals via their distribution. By the same argument as above we also see that $\|B_k^* B_k\|_{\infty,1} = \|A_k\|_{\infty}^2$. Plugging this into our formula for blocks (7) yields

$$\pi_k := \frac{\max \left\{ \max_{1 \leq \ell \leq \sqrt{K}} \left\{ \sum_{i=1}^{\sqrt{K}} |A_{k,i}|^2 W_{\ell,i} \right\}, \|A_k\|_{\infty}^2 \right\}}{L}, \quad (18)$$

where L is the normalisation constant. If instead of vertical lines one would take horizontal lines $B_k := A \otimes A_{k,:}$, we would get

$$B_k^* B_k = \begin{pmatrix} A_{k,:}^* A_{k,:} & \dots & 0 \\ \vdots & \ddots & \vdots \\ 0 & \dots & A_{k,:}^* A_{k,:} \end{pmatrix},$$

without any reordering. Hence in this case

$$\|D_{\sqrt{p'}} B_k^* B_k D_{\sqrt{p'}}\| = \max_{1 \leq \ell \leq \sqrt{K}} \sum_{i=1}^{\sqrt{K}} |A_{k,i}|^2 W_{i,\ell},$$

which amounts to taking the maximum over all columns of the matrix W . Plugging this back into our formula for blocks (7) yields

$$\pi_k := \frac{\max \left\{ \max_{1 \leq \ell \leq \sqrt{K}} \left\{ \sum_{i=1}^{\sqrt{K}} |A_{k,i}|^2 W_{i,\ell} \right\}, \|A_k\|_{\infty}^2 \right\}}{L}, \quad (19)$$

where L is again the normalisation constant.

6.5.2 VERTICAL FOURIER-HAAR LINES

We now apply the above analysis to the special case where $A = \mathcal{F}\Psi^*$ is the 1D Fourier-Haar transform. This yields that A_0 is the separable 2D Fourier-Haar transform². Let $p \in \mathbb{R}^K$ again be our weight vector and define the matrix $W \in \mathbb{R}^{\sqrt{K} \times \sqrt{K}}$ such that $\text{vec}(W) = p$. We again denote by M_{ℓ} the frequency bands of the one dimensional Fourier transform and by

2. In all other experiments we use non-separable 2D wavelet transforms.

Ω_ℓ the dyadic partition (see previous subsection). In the 2D setting we define the **average maximal sparsity in level ℓ** as

$$S_\ell := \max_k \|W_{k,\Omega_\ell}\|_1. \quad (20)$$

This is equivalent to the 1D case up to taking the maximum over all rows of the matrix W . Using (12) and assuming that $S_\ell > 1$ for all $1 \leq \ell \leq J$, the above analysis yields for $k \in M_j$

$$\|B_k^* D_p B_k\| = \max_{1 \leq \ell \leq \sqrt{K}} \sum_{i=1}^{\sqrt{K}} |A_{k,i}|^2 W_{\ell,i} \leq \sum_{i=1}^{\sqrt{K}} \max_{1 \leq \ell \leq \sqrt{K}} |A_{k,i}|^2 W_{\ell,i} \quad (21)$$

$$\lesssim 2^{-j} S_j + 2^{-j} \sum_{p \neq j} 2^{|j-p|} S_p, \quad (22)$$

and thus by using π as defined in (18) our main result yields the sufficient condition

$$m \gtrsim \left(\sum_j S_j + \sum_{p \neq j} 2^{|j-p|} S_p \right) \log^3(K/\varepsilon), \quad (23)$$

in line with results in [3]. Note that the first inequality in (21) is rather crude and potentially loses a lot of information about the relationship between the matrix W and the structure of the 2D Fourier-Haar matrix $A_0 = \mathcal{F}\Psi^*$. This is why in our experiments we will stick with the quantity $\|B_k^* D_p B_k\| = \max_{1 \leq \ell \leq \sqrt{K}} \sum_{i=1}^{\sqrt{K}} |A_{k,i}|^2 W_{\ell,i}$.

6.5.3 NUMERICAL EXPERIMENTS OF BLOCKS OF MEASUREMENTS FOURIER - DB4

In this subsection we will use blocks of measurements in numerical experiments— Figure 5. We conduct two experiments, first by measuring along horizontal lines in the 2D k-space (left column) and then by measuring square blocks of size 16×16 in the 2D k-space (middle column). We again use the Brain dataset with a threshold of around 0.023 to generate a estimate of the matrix W in the *separable* 2D DB4 wavelet basis (top right). Plugging these estimated weights into Formula (7) we get an adapted sampling distribution on the vertical lines (top left) and on the square blocks (top middle). Sampling 20% of measurements from the 2D k-space (middle row) we get good reconstruction of the reference image (bottom right) for both measurement techniques (bottom left and middle). This shows how our results also apply to the setting of blocks of measurements.

7. Discussion

The above results showed that the optimal variable density subsampling strategy in a compressed sensing setup should not only depend on the structure of the sensing and sparsity matrices, but also on the distribution of sparsity patterns of the signals to be measured. We derived lower bounds on the number of measurements to ensure recovery of the sparse signals with high probability and derived a simple formula for the optimal subsampling strategy. We showed that this distribution can be estimated from a training set and that the resulting adapted subsampling scheme provides state of the art performance in a range of situations. For future work it would be interesting to analyse different settings of blocks of measurements, where explicit lower bounds on the number of measurements can be derived.

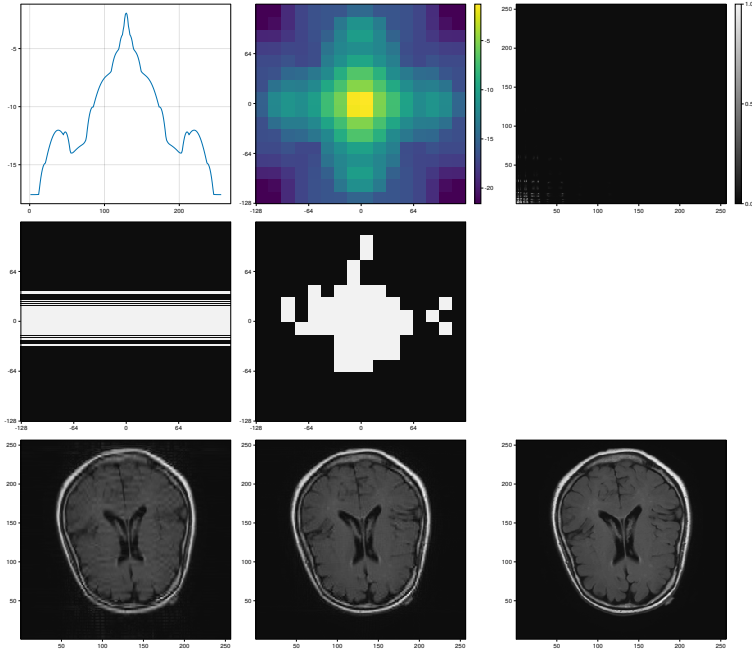


Figure 5: Adapted variable density sampling schemes with vertical lines (left column) and squares (middle column). Matrix W of sparse support distribution in the separable 2D DB4 wavelet basis (top right), test image (bottom right) and reconstructions (bottom left and middle). The resulting PSNR values are: Lines - 29.9 and Squares - 33.9.

Acknowledgements

This work was supported by the Austrian Science Fund (FWF) under Grant no. Y760. The author wants to thank Karin Schnass for proof-reading the manuscript and her insightful comments.

Appendix A. Proof of Theorem 3

Now we turn to proving Theorem 3. Note that we have three sources of randomness: the signs σ , the set of random measurements J and the random supports I . Strictly speaking, we are working on the product measure of the three, but in slight abuse of notation, we will write \mathbb{P}_σ , \mathbb{P}_J and \mathbb{P}_S to indicate the probability measure that we use for the corresponding concentration inequalities. The exact statement of Theorem 3 — including constants — reads as

Theorem 7 *Assume that m measurements B_k are sampled according to probabilities π_k and the signals follow the model in 2, where the support $I \subseteq \mathbb{K}$ is chosen according to the rejective*

sampling model with probabilities p_1, \dots, p_K such that $\sum_{k=1}^K p_k = S$ and $0 < p_k \leq 1$. If

$$\begin{aligned} m &\geq \max_k \frac{\|B_k^* B_k\|_{\infty,1}}{\pi_k} 384 \log^2(10^4 K/\varepsilon) \log(54K^2/\varepsilon), \quad \text{and} \\ m &\geq \max_k \frac{\|B_k D_p B_k^*\|_{2,2}}{\pi_k} 10^4 e^2 \log^2(10^4 K/\varepsilon), \end{aligned} \quad (24)$$

then (1) recovers the sparse signal with probability $1 - \varepsilon$.

Before we can state the proof, we need to establish 5 concentration inequalities. To that end, we define

$$\Lambda := \max_k \frac{\|B_k D_p B_k^*\|_{2,2}}{\pi_k m} \quad \text{and} \quad \kappa := \max_k \frac{\|B_k^* B_k\|_{\infty,1}}{\pi_k m}.$$

Further let $H := A^* A - \text{diag}(A^* A)$. We begin by bounding the biggest entry of H . For that we can apply the standard Bernsteins's inequality to each entry together with a unit bound to get

Lemma 8 *Let A depend on the draw of the j_ℓ . Then for all $t \geq 0$, we have*

$$\mathbb{P}_J (\|A^* A - \mathbb{I}\|_{\infty,1} \geq t) \leq 2K^2 \exp\left(-\frac{t^2/2}{\kappa(1+t)/3}\right). \quad (25)$$

Proof We fix indices i and j and bound the i, j -th entry of the matrix $A^* A - \mathbb{I}$. Recall that by definition of A

$$A^* A - \mathbb{I} = \sum_{k=1}^m \frac{1}{m} \left(\frac{B_{j_k}^* B_{j_k}}{\pi_{j_k}} - \mathbb{I} \right). \quad (26)$$

Focusing only on the i, j -th entry of this matrix, we can write this entry as $\sum_{k=1}^m x_k$, where $x_k := \frac{1}{m} e_j^* \left(\frac{B_{j_k}^* B_{j_k}}{\pi_{j_k}} - \mathbb{I} \right) e_i$. By definition $\mathbb{E}[x_k] = 0$ and we can bound each $x_k \leq \kappa$ for all k . To bound the variance, note

$$\mathbb{E}[x_k^2] = \mathbb{E} \left[\left(\frac{e_j^* B_{j_k}^* B_{j_k} e_i}{\pi_{j_k} m} \right)^2 \right] - \frac{1}{m^2} e_j^* \mathbb{I} e_i \leq \kappa \mathbb{E} \left[\frac{e_i^* B_{j_k}^* B_{j_k} e_i}{\pi_{j_k} m} \right] \leq \kappa \frac{1}{m}, \quad (27)$$

which leads to $\sigma^2 = \sum_{k=1}^m \mathbb{E}[x_k^2] \leq \kappa$. An application of the Bernstein inequality together with a union bound over all pairs i, j yields the result. \blacksquare

In the next step we want to bound the largest ℓ_2 -norm of the matrix $HD_{\sqrt{p}}$, i.e. we want to bound $\|HD_{\sqrt{p}}\|_{\infty,2}$. To that end we are going to apply the vector Bernstein inequality [22] together with a union bound. Concretely we have

Lemma 9 *Let I be a fixed support of cardinality S and let A depend on the draw of the j_ℓ . Then for all $t > 0$, we have*

$$\mathbb{P}_J \left(\max_i \|A_i^* A_{/i} D_{\sqrt{p}}\|_2 \geq t \right) \leq 28K \exp\left(-\frac{t^2/2}{\Lambda + \sqrt{\Lambda \kappa} \cdot t/3}\right).$$

Proof For a fixed i we set $D_{/i}$ the diagonal matrix that is one except for the i -th entry, where it is zero. For ease of notation we are going to look at the transposed vector $D_{\sqrt{p}}A_{/i}^*A_i$ which we can write as

$$\|D_{\sqrt{p}}D_{/i}A^*Ae_i\|_2 = \left\| \sum_{k=1}^m \frac{D_{\sqrt{p}}D_{/i}B_{j_k}^*B_{j_k}e_i}{\pi_{j_k}m} \right\|_2 = \left\| \sum_{k=1}^m X_k \right\|_2,$$

where

$$X_k := \frac{D_{\sqrt{p}}D_{/i}B_{j_k}^*B_{j_k}e_i}{\pi_{j_k}m}.$$

By definition we have $\mathbb{E}[X_k] = \frac{1}{m}D_{\sqrt{p}}D_{/i}\sum_{\ell=1}^M B_\ell B_\ell^*e_i = \frac{1}{m}D_{\sqrt{p}}D_{/i}e_i = 0$. Further

$$\max_k \|X_k\|_2 = \max_k \left\| \frac{D_{\sqrt{p}}B_k^*B_k e_i}{\pi_k m} \right\|_2 \leq \sqrt{\Lambda\kappa}$$

To bound the variance, note that

$$\mathbb{E}[\|X_k\|_2^2] = \mathbb{E} \left[\left\| \frac{D_{\sqrt{p}}B_{j_k}^*B_{j_k}e_i}{\pi_{j_k}m} \right\|_2^2 \right] \leq \Lambda \mathbb{E} \left[\left\| \frac{B_{j_k}e_i}{\sqrt{\pi_{j_k}m}} \right\|_2^2 \right] = \Lambda \|e_i\|_2^2 \frac{1}{m} = \frac{\Lambda}{m}.$$

This leads to $\sigma^2 = \sum_{k=1}^m \mathbb{E}[\|X_k\|_2^2] \leq \Lambda$. An application of the vector Bernstein inequality [22] together with an union bound finishes the proof. \blacksquare

Next we show how to bound the operator norm of the matrix $D_{\sqrt{p}}HD_{\sqrt{p}}$. The following result is similar to standard results in CS theory [9, Lemma 2.1] and [6, Lemma C.1]. The Matrix Bernstein inequality [30] yields

Lemma 10 *Let A depend on the draw of the j_ℓ . Then for all $t \geq 0$, we have*

$$\mathbb{P}_J (\|D_{\sqrt{p}}A^*AD_{\sqrt{p}} - \text{diag}(A^*A)D_p\|_{2,2} \geq t) \leq 2K \exp \left(-\frac{t^2/2}{4\Lambda(1+t)/3} \right).$$

Proof We begin by noting that we can write

$$\begin{aligned} D_{\sqrt{p}}HD_{\sqrt{p}} &= D_{\sqrt{p}}A^*AD_{\sqrt{p}} - \text{diag}(A^*A)D_p \\ &= \sum_{k=1}^m \left(\frac{D_{\sqrt{p}}B_{j_k}^*B_{j_k}D_{\sqrt{p}}}{\pi_{j_k}m} - \text{diag} \left(\frac{B_{j_k}^*B_{j_k}}{\pi_{j_k}m} \right) D_p \right) = \sum_{k=1}^m X_k, \end{aligned} \quad (28)$$

where $X_k := \left(\frac{D_{\sqrt{p}}B_{j_k}^*B_{j_k}D_{\sqrt{p}}}{\pi_{j_k}m} - \text{diag} \left(\frac{B_{j_k}^*B_{j_k}}{\pi_{j_k}m} \right) D_p \right)$. By definition of the j_k we have $\mathbb{E}[X_k] = 0$. Further

$$\|X_k\|_{2,2} \leq 2 \max_k \frac{\|D_{\sqrt{p}}B_k^*B_kD_{\sqrt{p}}\|_{2,2}}{\pi_k m} = 2\Lambda.$$

Using that for two discrete symmetric random matrices A and B over the same probability space that we have [25]

$$\|\mathbb{E}[(A+B)(A+B)^*]\| \leq \left(\|\mathbb{E}[A^2]\|_{\frac{1}{2}} + \|\mathbb{E}[B^2]\|_{\frac{1}{2}} \right)^2. \quad (29)$$

Using this to bound the variance we get

$$\|\mathbb{E}[X_k^2]\| \leq 4\|\mathbb{E}\left[\left(\frac{D_{\sqrt{p}}B_{j_k}^*B_{j_k}D_{\sqrt{p}}}{\pi_{j_k}m}\right)^2\right]\| \leq 4\Lambda\frac{1}{m},$$

which leads to $\sigma^2 = \|\sum_{k=1}^m \mathbb{E}[X_k^2]\|_{2,2} \leq 4\Lambda$. An application of the Matrix Bernstein inequality yields the result. \blacksquare

We further need the following Hoeffding-like tail bound for sums of centered complex random variables — see ([15] Corollary 7.21 and Corollary 8.10).

Lemma 11 *Let $M \in \mathbb{C}^{K \times S}$ be a matrix and $x \in \mathbb{R}^S$ such that $\text{sign}(x_i) \in \mathbb{R}^S$ is an independent Rademacher sequence. Then, for all $t \geq 0$*

$$\mathbb{P}_\sigma(\|Mx\|_\infty \geq t) \leq 2K \exp\left(-\frac{t^2}{2\|M\|_{\infty,2}^2\|x\|_\infty^2}\right).$$

The following concentration inequality can be found in [26] and follows from a decoupling argument followed by an application of the standard Chernoff inequality and a union bound.

Lemma 12 ([26, Lemma 3.4]) *Let $H \in \mathbb{C}^{K \times K}$ be some matrix. Assume $I \subseteq \mathbb{K}$ is chosen according to the rejective sampling model with probabilities p_1, \dots, p_K such that $\sum_{i=1}^K p_i = S$. Further let p denote the corresponding weight vector. Then, for all $v > 0$*

$$\mathbb{P}_S(\|H_I\|_{\infty,2} \geq v) \leq 2K \left(e \frac{\|HD_{\sqrt{p}}\|_{\infty,2}^2}{v^2} \right)^{\frac{v^2}{\|H\|_{\infty,1}^2}}.$$

The key ingredient to prove Theorem 3 is the following concentration inequality for the operator norm of random submatrices with non-uniformly distributed supports which can be found in [26]³. This is what allows us to go one step further than existing results in analysing the underlying relationship between the sensing matrix and the distribution of sparse supports.

Lemma 13 ([26, Theorem 3.1]) *Let $H \in \mathbb{C}^{K \times K}$ be a matrix with zero diagonal. Assume that the support $I \subseteq \mathbb{K}$ is chosen according to the rejective sampling model with probabilities p_1, \dots, p_K such that $\sum_{i=1}^K p_i = S$. Further let p denote the corresponding weight vector. If $t \geq 2e^2\|D_{\sqrt{p}}HD_{\sqrt{p}}\|_{2,2}$, then*

$$\mathbb{P}(\|H_{I,I}\|_{2,2} \geq t) \leq 216K \exp\left(-\min\left\{\frac{t^2}{4e^2\|HD_{\sqrt{p}}\|_{\infty,2}^2}, \frac{t}{2\|H\|_{\infty,1}}\right\}\right). \quad (30)$$

With all of these concentration inequalities in place we are finally able to prove Theorem 3.

Proof From [29, 16] we know that if $\|A_{I^c}^*A_I(A_I^*A_I)^{-1}\sigma_I\|_\infty < 1$, then x is the unique solution of the ℓ_1 -minimisation problem (1). Set $M := A_{I^c}^*A_I(A_I^*A_I)^{-1}$ and assume that $\|A_I^*A_I - \mathbb{I}\| \leq 1/2$. Then

$$\|M\|_{\infty,2} = \|A_{I^c}^*A_I(A_I^*A_I)^{-1}\|_{\infty,2} \leq \|A_{I^c}^*A_I\|_{\infty,2}\|(A_I^*A_I)^{-1}\|_{2,2} \leq 2\|A_{I^c}^*A_I\|_{\infty,2}.$$

3. The result in the cited paper is stated only for real matrices, but a careful analysis of the proof shows that this result also holds for complex matrices.

Noting that $\|A_{I^c}^* A_I\|_{\infty,2} = \max_{i \in I^c} \|A_I^* A_i\|_2$ we have

$$\begin{aligned} \mathbb{P}(\|M\sigma\|_{\infty} \geq 1) &\leq \mathbb{P}_{\sigma}(\|M\sigma\|_{\infty} \geq 1 \mid \|M\|_{\infty,2} \leq 2\gamma) \\ &\quad + \mathbb{P}(\|A_I^* A_I - \mathbb{I}\|_{2,2} \geq 1/2) + \mathbb{P}\left(\max_{i \in I^c} \|A_I^* A_i\|_2 \geq \gamma\right). \end{aligned}$$

Setting $\gamma^2 = \frac{1}{8 \log(6K/\varepsilon)}$ and applying Lemma 11 to $M\sigma$ yields that the first term on the right hand side is bound by $\varepsilon/3$. We denote by $J := (j_1, \dots, j_m)$ the m -dimensional vector that selects which blocks of measurements are taken. Setting $H := A^* A - \text{diag}(A^* A)$ we see that H depends on the random sequence J . With that in mind we define

$$\mathcal{J} := \{J \mid \|H\|_{\infty,1} \leq v_1, \|HD_{\sqrt{p}}\|_{\infty,2}^2 \leq v_2, \|D_{\sqrt{p}} H D_{\sqrt{p}}\|_{2,2} \leq v_3\} \quad (31)$$

to be the collection of sequences J that satisfy the above conditions. Further

$$\begin{aligned} &\mathbb{P}(\|A_I^* A_I - \mathbb{I}\|_{2,2} \geq 1/2) + \mathbb{P}\left(\max_{i \in I^c} \|A_I^* A_i\|_2 \geq \gamma\right) \\ &\leq \mathbb{P}_S(\|A_I^* A_I - \text{diag}(A_I^* A_I)\|_{2,2} \geq 1/4 \mid \mathcal{J}) + \mathbb{P}_J(\mathcal{J}) \\ &\quad + \mathbb{P}\left(\|\text{diag}(A_I^* A_I) - \mathbb{I}\|_{2,2} \geq 1/4\right) \\ &\quad + \mathbb{P}_S\left(\max_{i \in I^c} \|A_I^* A_i\|_2 \geq \gamma \mid \mathcal{J}\right) + \mathbb{P}_J(\mathcal{J}) \end{aligned} \quad (32)$$

By Lemma 12 and Lemma 13 we can bound the two conditional probabilities via (for v_3 defined as below)

$$\begin{aligned} &\mathbb{P}_S(\|A_I^* A_I - \text{diag}(A_I^* A_I)\|_{2,2} \geq 1/4 \mid \mathcal{J}) + \mathbb{P}_S\left(\max_{i \in I^c} \|A_I^* A_i\|_2 \geq \gamma \mid \mathcal{J}\right) \\ &\leq 216K \exp\left(-\min\left\{\frac{(1/4)^2}{4e^2 v_2^2}, \frac{1/4}{2v_1}\right\}\right) + 2K \left(e \frac{v_2^2}{\gamma^2}\right)^{\frac{\gamma^2}{v_1}}. \end{aligned} \quad (33)$$

Setting

$$\begin{aligned} v_1 &:= \frac{1}{8 \log(216 * 6K/\varepsilon)} \\ v_2 &:= \frac{1}{8e \log^{1/2}(216 * 6K/\varepsilon)} \\ v_3 &:= \frac{1}{8e^2} \end{aligned} \quad (34)$$

we get that (33) is smaller than $\varepsilon/3$. Plugging this into (32) we see that to finish the proof we have to show that $\mathbb{P}\left(\|\text{diag}(A_I^* A_I) - \mathbb{I}\| \geq 1/4\right) + 2\mathbb{P}(\mathcal{J}) \leq \varepsilon/3$. Using Lemmas 9, 8 and 10 to bound the three terms in \mathcal{J} we get

$$\begin{aligned} &\mathbb{P}\left(\|\text{diag}(A_I^* A_I) - \mathbb{I}\|_{2,2} \geq 1/4\right) + 2\mathbb{P}_J(\mathcal{J}) \leq 6K^2 \exp\left(-\frac{v_1^2/2}{\kappa(1+v_1)/3}\right) \\ &\quad + 56K \exp\left(-\frac{v_2^2/2}{\Lambda + \sqrt{\Lambda\kappa} \cdot v_2/3}\right) + 4K \exp\left(-\frac{v_3^2/2}{4\Lambda(1+v_3)/3}\right) \\ &\leq 6K^2 \exp\left(-\frac{v_1^2}{4\kappa}\right) + 56K \exp\left(-\frac{v_2^2}{4\Lambda}\right) + 4K \exp\left(-\frac{v_3^2}{2.72\Lambda}\right). \end{aligned} \quad (35)$$

By the assumptions on Λ and κ we indeed have $3\mathbb{P}_J(\mathcal{J}) \leq \varepsilon/3$ which finishes the proof.

Remark 14 *The proof of our main result relies heavily on the random signs of our signals. One could remove this assumption by instead employing the so-called "golfing scheme" proposed in [17]. Following the argument in [9] one should be able to derive similar results in the case of deterministic sign patterns. Since this would not have any impact on the optimal sampling distribution we opted for the shorter proof presented here.*

■

References

- [1] B. Adcock, A.C. Hansen, and B. Roman. A note on compressed sensing of structured sparse wavelet coefficients from subsampled fourier measurements. *IEEE Signal Processing Letters*, 23(5):732–736, 2016.
- [2] B. Adcock, A.C. Hansen, C. Poon, and B. Roman. Breaking the coherence barrier: A new theory for compressed sensing. *Forum of Mathematics, Sigma*, 5:e4, 2017.
- [3] B. Adcock, C. Boyer, and S. Brugiapaglia. On oracle-type local recovery guarantees in compressed sensing. *Information and Inference: A Journal of the IMA*, 10(1):1–49, 2020.
- [4] S. Becker, J. Bobin, and E. Candès. NESTA: A fast and accurate first-order method for sparse recovery. *SIAM Journal on Imaging Sciences*, 4(1):1–39, 2011.
- [5] J. Bigot, C. Boyer, and P. Weiss. An analysis of block sampling strategies in compressed sensing. *IEEE Transactions on Information Theory*, 62, 05 2013.
- [6] C. Boyer, P. Weiss, and J. Bigot. Compressed sensing with structured sparsity and structured acquisition. *Applied and Computational Harmonic Analysis*, 46(2):312 – 350, 2019.
- [7] M. Buda. Brain MRI segmentation. <https://www.kaggle.com/datasets/mateuszbuda/lgg-mri-segmentation>, 2019. Accessed: 2022-06-27.
- [8] E. Candès, J. Romberg, and T. Tao. Robust uncertainty principles: exact signal reconstruction from highly incomplete frequency information. *IEEE Transactions on Information Theory*, 52(2):489–509, 2006.
- [9] E. J. Candes and Y. Plan. A probabilistic and ripless theory of compressed sensing. *IEEE Transactions on Information Theory*, 57(11):7235–7254, 2011.
- [10] N. Chauffert, P. Ciuciu, J. Kahn, and P. Weiss. Variable density sampling with continuous trajectories. *SIAM Journal on Imaging Sciences*, 7, 11 2013.
- [11] N. Chauffert, P. Ciuciu, and P. Weiss. Variable density compressed sensing in MRI. Theoretical vs heuristic sampling strategies. In *2013 IEEE 10th International Symposium on Biomedical Imaging*, pages 298–301, 2013.

- [12] I.Y. Chun and B. Adcock. Compressed sensing and parallel acquisition. *IEEE Transactions on Information Theory*, 63(8):4860–4882, 2017.
- [13] D.L. Donoho. Compressed sensing. *IEEE Transactions on Information Theory*, 52(4):1289–1306, 2006.
- [14] D.L. Donoho, M. Elad, and V.N. Temlyakov. Stable recovery of sparse overcomplete representations in the presence of noise. *IEEE Transactions on Information Theory*, 52(1):6–18, January 2006.
- [15] S. Foucart and H. Rauhut. *A Mathematical Introduction to Compressive Sensing*. Applied and Numerical Harmonic Analysis. Birkhäuser, 2013.
- [16] J. Fuchs. On sparse representations in arbitrary redundant bases. *IEEE Transactions on Information Theory*, 50:1341–1344, 2004.
- [17] D. Gross. Recovering low-rank matrices from few coefficients in any basis. *IEEE Transactions on Information Theory*, 57(3):1548–1566, 2011.
- [18] J. Hajek. Asymptotic theory of rejective sampling with varying probabilities from a finite population. *Annals of Mathematical Statistics*, 35(4):1491–1523, 1964.
- [19] H. HRauhut. *Compressive Sensing and Structured Random Matrices*, pages 1–92. De Gruyter, Berlin, New York, 2010.
- [20] F. Kraher and R. Ward. Stable and robust sampling strategies for compressive imaging. *arXiv:1210.2380*, 2012.
- [21] C. Li and B. Adcock. Compressed sensing with local structure: Uniform recovery guarantees for the sparsity in levels class. *Applied and Computational Harmonic Analysis*, 46(3):453–477, 2019.
- [22] S. Minsker. On some extensions of Bernstein’s inequality for self-adjoint operators. *Statistics and Probability Letters*, 127:111–119, 2017.
- [23] Y. Nesterov. Smooth minimization of nonsmooth functions. *Math. Programming*, pages 127–152, 2005.
- [24] G. Puy, P. Vandergheynst, and Y. Wiaux. On variable density compressive sampling. *IEEE Signal Processing Letters*, 18(10):595–598, 2011.
- [25] S. Ruetz. *Compressed Sensing and Dictionary Learning with Non-Uniform Support Distribution*. PhD thesis, University of Innsbruck, 2022.
- [26] S. Ruetz and K. Schnass. Submatrices with non-uniformly selected random supports and insights into sparse approximation. *SIAM Journal on Matrix Analysis and Applications*, 42(3):1268–1289, 2021.
- [27] S. Ruetz and K. Schnass. Non-asymptotic bounds for inclusion probabilities in rejective sampling, 2022.

- [28] Stanford ML group. MRNet Dataset. <https://stanfordmlgroup.github.io/competitions/mrnet/>, 2019. Accessed: 2022-06-27.
- [29] J. Tropp. Recovery of short, complex linear combinations via l1 minimization. *IEEE Transactions on Information Theory*, 51:1568–1570, 2005.
- [30] J. Tropp. User-friendly tail bounds for sums of random matrices. *Foundations of Computational Mathematics*, 12(4):389–434, 2012.